JOURNAL OF SPACECRAFT AND ROCKETS
Vol. 29, No. 2, March-April 1992

# Solar System "Fast Mission" Trajectories Using Aerogravity Assist

James E. Randolph* and Angus D. McRonald†
*Jet Propulsion Laboratory, California Institute of Technology, Pasadena, California 91109*

**Initial analyses of the aerogravity assist (AGA) delivery technique to solar system targets (and beyond) has been encouraging. Mission opportunities are introduced that do not exist with typical gravity assist trajectories and current launch capabilities. The technique has the most payoff for high-energy missions such as outer planet orbiters and flybys. The goal of this technique is to reduce the flight duration significantly and to eliminate propulsion for orbit insertion. The paper will discuss detailed analyses and parametric studies that consider launch opportunities for missions to the Sun, Saturn, Uranus, Neptune, and Pluto using AGA at Venus and Mars.**

## Nomenclature

| | |
|---|---|
| $A$ | = reference area of vehicle |
| $C_D$ | = drag coefficient |
| $C_L$ | = lift coefficient |
| $DV$, $\Delta V$ | = velocity increment |
| $L/D$ | = ratio of lift to drag (also $C_L/C_D$) |
| $m$ | = mass of vehicle |
| $R$ | = flyby radius |
| $V$ | = velocity of vehicle |
| $\theta$ | = departure angle of $V_\infty$ vector relative to planet velocity vector |
| $\rho$ | = atmospheric density |
| $\phi$ | = arc length in atmosphere, bending angle at planet |

*Subscripts*

| | |
|---|---|
| $c$ | = circular orbit |
| $E$ | = Earth |
| esc | = escape |
| $H$ | = heliocentric |
| $M$ | = Mars |
| $p$ | = periapsis or planet |
| $S$ | = Saturn |
| $s/c$ | = spacecraft |
| $V$ | = Venus |
| $\infty$ or inf | = relative to planet at infinity |

## Introduction

IN three prior papers[1-3] the authors studied the use of aerogravity-assist (AGA) maneuvers at Venus and Mars with relevance to three classes of missions: 1) a mission of the solar probe type that seeks to achieve a polar orbit with perihelion at about 4 solar radii ($4R_s$), 2) high-speed missions to the outer planets and beyond with relatively short travel times, and 3) fast Earth-return trajectories from Mars. Two important conclusions were reached in the papers: 1) it is better to perform a two-planet (i.e., Venus, Mars) AGA mission if very high energy missions are required because the launch energy is lower, and 2) it is better to perform the final AGA maneuvers at Mars rather than at Venus because the Mars heliocentric velocity is lower and thus the required $V_{inf}$ and the AGA periapsis velocity are also lower.

One of the problems of AGA maneuvers in the atmospheres of the terrestrial planets is that most mission objectives call for high-speed maneuvers in a high molecular weight (MW) gas (MW = 44 for carbon dioxide at Mars and Venus). This speed often exceeds the present technology limit for computation of heat transfer and thermal response, believed to be about 15 km/s for high MW atmospheres. A further problem at high speeds is the aeroload on the structure, as large as 10–20 Earth $g$.

In a previous paper[3] AGA possibilities at Saturn using the atmosphere of Titan were analyzed and will be discussed here in the context of a more complete interplanetary mission. A high-speed trajectory to Pluto will also be discussed.

New analyses in this paper explore in some detail the trajectory constraints and opportunities for missions to the outer planets, particularly Saturn, Uranus, and Neptune, using AGA maneuvers at Venus and Mars in sequence and restricting the AGA atmospheric speeds at Venus and Mars to about 15 km/s. This value of 15 km/s was adopted arbitrarily as a technology development goal to illustrate the celestial mechanics possibilities of AGA at this speed. Current flight experience for high-speed atmospheric entry is from Apollo at about 10.7 km/s.

## AGA Concept

Figure 1 represents an aerogravity-assist maneuver[2] in a planetary atmosphere, showing how flight in the atmosphere is used to augment the natural gravitational bending of the flight path. The planet-relative flight path using AGA is shown being steadily rotated as the vehicle flies in the atmosphere, balancing the "centrifugal" force with aerodynamic lift directed downwards, and exits, by reversing the lift vector, when the appropriate degree of turn has been reached. Note that the turn need not be in the original plane of motion, i.e., an AGA can be used for plane change maneuvers. Also, there is an inevitable loss of hyperbolic velocity ($V_{inf}$) relative to the planet in the gliding AGA flight. Recent research with high-lift hypersonic vehicles such as waveriders[4-6] suggests that the velocity losses in the atmosphere can be minimized with this type of vehicle. A high $L/D$ vehicle is required for successful AGA maneuvers, and the waverider is therefore a strong candidate. Moreover, the bow shock is attached over the entire surface, and the high sweep back reduces the leading-edge heating. The stagnation temperature for a blunt body at high hypersonic speed is known to exceed the operating temperature of all current materials. To reject the heat, a heat shield would be

Presented as Paper 91-0531 at the AIAA 29th Aerospace Sciences Meeting, Reno, NV, Jan. 7-10, 1991; received May 24, 1991; revision received Aug. 30, 1991; accepted for publication Sept. 3, 1991. 

*Solar Probe Study Manager. Associate Fellow AIAA.
†Member of the Technical Staff. Member AIAA.

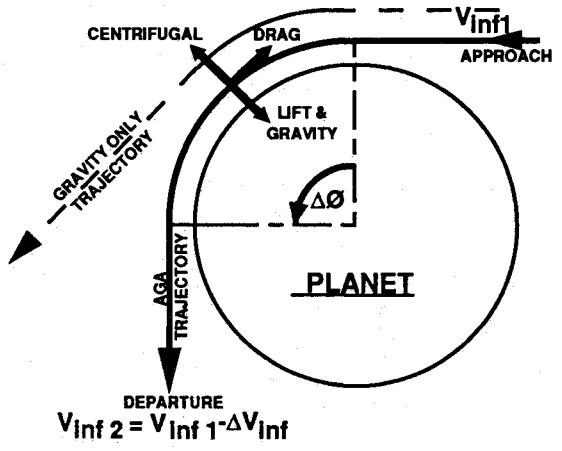


**Fig. 1 Aerogravity-assist maneuver in a planetary atmosphere.**

used that might employ ablation, radiation outwards at high temperatures, and convective/conductive internal cooling (passive and active). It is expected that the nose and the leading edges of a waverider would have to be blunted slightly to reduce the convective heating rate in high-speed AGA maneuvers, and heat rejection would have to be accounted for. This blunting of the leading edge would detract somewhat from the high $L/D$ of a waverider with sharp leading edges. However, it is expected that the operational problems of AGA (navigation, flight control, heat rejection) could be resolved with minimum technology development for speeds that may be as high as the 15 km/s adopted here.

It should be noted that the use of a high $L/D$ vehicle and AGA reduces the launch $C_3$ requirements greatly, i.e., increases the possible spacecraft launch mass. However, an interplanetary spacecraft must now fit into a high $L/D$ vehicle and provision made for heat rejection, control, trajectory correction, etc. The result may well be a total mass comparable with the launch mass without AGA, but the AGA case has the advantage of greatly reduced travel time, more capability at the planetary destination, and more frequent launch opportunities as will be discussed later.

The AGA maneuver as expressed in velocity vector space in heliocentric coordinates is illustrated in Fig. 2. The vectors $V_p$ and $V_{s/c}$ represent the heliocentric velocities of the planet and the spacecraft, respectively, and $V_\infty$ represents the hyperbolic excess velocity of the spacecraft relative to the planet. These vectors satisfy the vector equation $V_{s/c} = V_p + V_\infty$. Aerogravity assist can be used to decrease or increase a spacecraft's heliocentric velocity depending on whether it is desired to travel toward or away from the Sun. For example, the objective of the AGA maneuver at Mars for the solar probe mission (as illustrated in Fig. 2a) is to reduce the $V_{s/c}$ to nearly zero by rotating the $V_\infty$ vector toward the $V_p$ vector as shown, i.e., performing an AGA maneuver with a large bending angle in a retrograde sense. On the other hand, Fig. 2b shows the $V_\infty$ vector in direct rotation so as to add to the heliocentric velocity for a flight to the outer planets. Thus, the AGA concept introduces a controllable parameter, the AGA bending angle $\phi$ at the planet, which has significant implications for changing the heliocentric velocity of the spacecraft during gravity-assist (GA) maneuvers.

An approximate analysis[2] resulted in a set of equations governing the centrifugal acceleration, the atmospheric density at which to perform the AGA, the periapsis speed, and the velocity loss in an AGA. The principal results from this analysis at radius $R$ require that atmospheric density, almost independent of the speed, at which the vehicle should fly is

$$\rho = \left[1 - \left(\frac{V_c}{V_p}\right)^2\right] \frac{2}{R}\left(\frac{m}{C_L A}\right) \tag{1}$$

In addition, we can write the drag loss equation:

$$\frac{\Delta V_\infty}{V_\infty} = -\frac{\phi}{(C_L/C_D)}\left[1 + \left(\frac{V_c}{V_\infty}\right)^2\right] \tag{2}$$

These equations assume equilibrium flight at constant $L/D$, thus requiring a slight increase in atmospheric density as velocity decreases during the AGA maneuver. It should be noted that the velocity loss is inversely proportional to the lift/drag ratio ($L/D$) of the vehicle, and this ratio must be high ($>5$) for AGA to be a viable concept. Also, Eq. (2) is linearized for small $\Delta V/V$. For larger $\Delta V/V$ the right side of the equation (RSE) becomes $1 - \exp(\text{RSE})$. For example, with $V_\infty = 10$ km/s at Venus, where $V_c = 7.3$ km/s, Eq. (2) would give $\Delta V_\infty/V_\infty = 0.307$ for $\phi = 1$ rad and $L/D = 5$, if $\Delta V_\infty = 3.07$ km/s during the AGA maneuver. With $V_\infty = 7$ at Mars ($V_c = 3.55$ km/s), Eq. (2) gives $V_\infty/V_\infty = 0.252$ for $\phi = 1$ rad and $L/D = 5$, if $\Delta V_\infty = 1.76$ km/s.

It was found in a previous paper[1] that a vehicle with $m/C_L A = 50$ kg/m$^2$ would require a $\rho$ value of about 1.5E−05 kg/m$^3$ for Earth, equivalent to the standard atmosphere at 83 km altitude. The same vehicle at Mars (with $R = 3460$ instead of 6460 km) would require $\rho = 2.9\text{E}-05$ kg/m$^3$, i.e., a height of 61 km, well above the highest mountains. For Venus with $R = 6150$ km the value of $\rho$ would be 1.6E−05 kg/m$^3$, at an altitude of about 104 km.

## Solar Probe Trajectory Using AGA

The intent of Ref. 1 was to find an AGA trajectory to the Sun using only a Venus AGA (VAGA) maneuver. A solar probe mission requires that the heliocentric velocity of the spacecraft must be virtually reduced to zero to cause the spacecraft to "fall" into the sun. If a planetary gravity-assist maneuver were to accomplish this, then the hyperbolic excess velocity ($V_\infty$) at the planet would be equal to the planet's heliocentric velocity, and the $V_\infty$ vector must be rotated through whatever angle is necessary to cancel the heliocentric velocity. To reach a 4 solar radii perihelion, the results of VAGA trajectory analysis required a launch energy ($C_3$) of greater than 200 km$^2$/s$^2$ and a Venus periapsis velocity of greater than 30 km/s. These were considered to be well beyond current capability and foreseeable technology advancements.

A subsequent paper[2] introduced the Venus AGA-Mars AGA (VAGAMAGA) trajectories that reduced both the launch energy and planetary periapsis velocity requirements. A VAGA-MAGA trajectory to the Sun resulting from the analysis is shown in Fig. 3. This analysis was unconstrained in terms of periapsis (atmospheric) velocity and assumed no velocity loss in the atmosphere (i.e., utilizing a very high $L/D \sim 10$ vehicle).

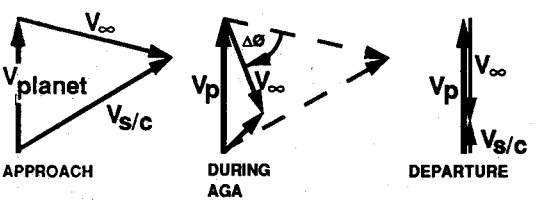


**a) Decrease velocity (e.g., solar probe)**

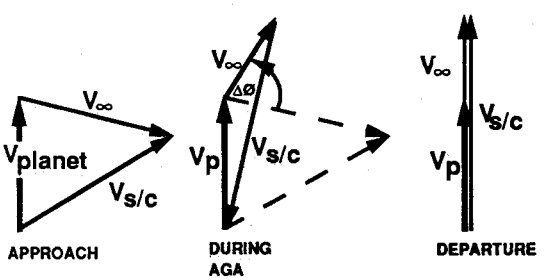


**b) Increase velocity (e.g., outer planets mission)**

**Fig. 2 Aerogravity-assist velocity vector geometry.**

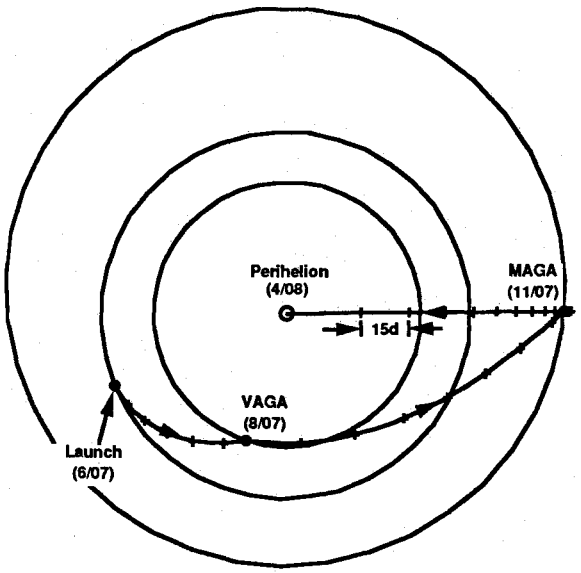


Fig. 3 Venus-Mars (VAGAMAGA) trajectory to the sun.

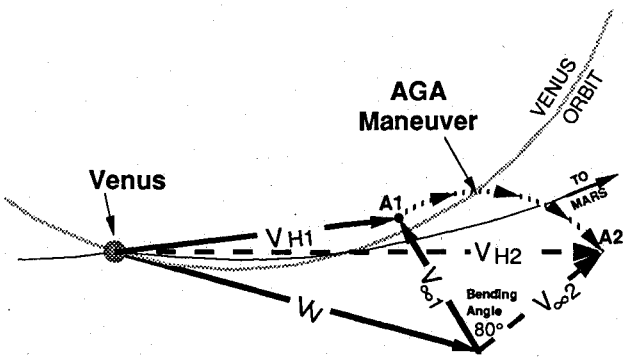


Fig. 4 Venus AGA (VAGA) maneuver geometry.

It was assumed at that time that these effects would not be significant enough to change the concept.

Details of the VAGA maneuver on the VAGAMAGA trajectory are shown in Fig. 4. Here the goal is to increase the heliocentric spacecraft velocity $V_H$ to allow the highest approach velocity at Mars. The initial velocity vector triangle is shown as solid lined vectors satisfying the relationship $V_H = V_V + V_\infty$. Note that the actual spacecraft trajectory approaching the planet, the spacecraft trajectory leaving the planet, and the planet's orbit are also shown in the figure. In addition, the velocity triangle is displayed as solid lined vectors before the AGA maneuver and dashed lined vectors after the maneuver. The VAGA maneuver is illustrated by the locus of point A, which is the intersection of the $V_H$ and $V_\infty$ vectors. The total bending angle $V_\infty$ (including aero and gravitational bending) for this maneuver is about 80 deg. Note that the $\Delta V$ gained by the spacecraft is the vector difference $V_{H2} - V_{H1}$ or about 19 km/s.

The details of the Mars aerogravity-assist (MAGA) maneuver are illustrated in Fig. 5. Here the spacecraft heliocentric velocity $V_H$ is to be reduced to virtually zero, allowing the spacecraft to "fall" into the Sun to accomplish the solar probe mission. The MAGA maneuver can be depicted by the locus of point B (i.e., from B1 to B2), which rotates the $V_\infty$ vector through an angle of about 83 deg during the maneuver. As in Fig. 2, the solid lines are the initial vector diagram and the only remnant of the final vector diagram is the $V_{\infty 2}$ vector shown as a dashed line. Note that $V_{H2}$ is reduced to near zero by the maneuver. The velocity lost (about 24 km/s) by the spacecraft is identical to the approach velocity $|V_{H1}|$. Velocity drag losses in the atmosphere would present a serious problem to this type of mission because the magnitude of $V_{\infty 2}$ must be nearly equal to the planet velocity $V_M$. Thus, $V_{\infty 1}$ must be greater than $V_{\infty 2}$ by the amount of the velocity loss. This could be a formidable requirement for an already extremely high velocity in the atmosphere of Mars (>25 km/s). The heating problems at this speed cannot be dismissed as trivial. Nevertheless, if the technology were to be developed, this technique would provide significant advantages (no particle radiation damage, short duration, and low final orbital period) over the typical Jupiter gravity-assist trajectory to the Sun.

## VAGAMAGA Trajectory to Pluto

The VAGAMAGA technique can also be applied to outbound trajectories with the same unconstrained assumptions at Venus and Mars. The high approach velocity at Mars can result in a large increase in a spacecraft's heliocentric velocity toward the outer planets. The large velocity leaving Mars on a VAGAMAGA trajectory can significantly reduce the trip time to Pluto as shown in Fig. 6. A duration of about 5 yr would be possible as compared with a typical Jupiter gravity-assist trajectory which would take about 15 yr. The trajectory shown would be launched in 2013 and arrive in 2018. This arrival date at Pluto is interesting in that the spacecraft velocity vector would have a heliocentric longitude of about 290 deg, only 20 deg away from the solar apex (270 deg). This direction is of interest to the interstellar probe scientific community. Another interesting point is that the atmospheric density value appropriate for AGA is about $1-2E-05$ kg/m$^3$, a value that is

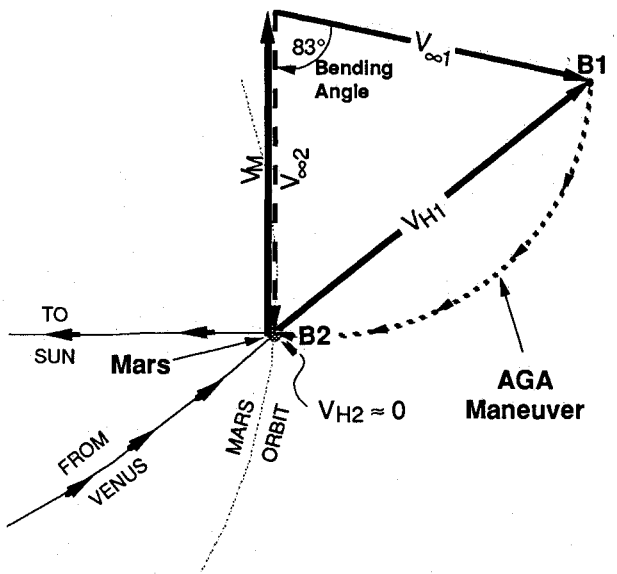


Fig. 5 Mars AGA (MAGA) maneuver geometry.

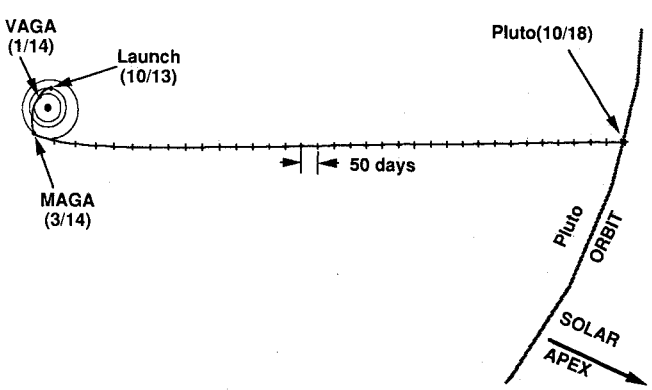


Fig. 6 VAGAMAGA trajectory to Pluto.

about one tenth the estimated[7] surface value of the atmosphere of Pluto, which is thought to be decreasing as Pluto moves towards its aphelion. It would seem that AGA at Pluto could be done early in the next century, so that a spacecraft could be aerocaptured into orbit or be redirected using an aerogravity-assist maneuver.

## VAGAMAGA Trajectory to Saturn

Another unconstrained trajectory going to Saturn, studied in these early analyses, is shown in Fig. 7. This VAGAMAGA trajectory to Saturn uses the same launch opportunity as the solar probe trajectory (2007) except that the bending angle is not retrograde at Mars. The direct trajectory at Mars allows a $\Delta V$ of greater than 24 km/s at Mars. Note that the flight duration is about 2 yr from launch to Saturn.

Once at Saturn, the atmosphere of the satellite Titan can be used for orbit modification or Titan aerogravity-assist (TAGA) maneuvers. Various TAGA maneuvers are possible as shown in Fig. 8. By changing the time of arrival and aiming point at Saturn (using midcourse maneuvers in deep space), different Titan relative geometries are possible as shown in the figure. Four typical geometries are depicted and are labeled Titan A, Titan B, etc. Each geometry contains a velocity triangle (satisfying the relationship $V_S = T_S + V_\infty$) similar to the AGA triangle at the planets as discussed before, but the coordinate system for this triangle is Saturn centered. It is assumed that the spacecraft approaches Saturn with a relatively high speed at Titan's orbit as shown by the horizontal vector $V_S$ in each Titan diagram. The Titan orbital velocity ($T_S$ vector) is about 5 km/s. Note that the $T_S$ vector changes orientation relative to the $V_S$ vector for each position in Titan's orbit. These different orientations suggest different mission characteristics that were discussed at length previously.[3] For example, if the maximum reduction of the $V_S$ were required, then the Titan A conditions would apply. Here the TAGA maneuver could rotate the $V_\infty$ vector (in a direction opposite to that shown by $\phi$) nearly 180 deg as shown by the resulting $V_{\infty 3}$ vector. (Note that in this and in all cases the locus of the tip of the $V_\infty$ vector describes a spiral of reducing radius, as the rotation angle gets larger, due to velocity loss caused by drag.) As the bending angle $\phi$ approaches 180 deg, the magnitude of $V_S$ (i.e., $V_{S3}$) approaches zero, allowing two possibilities. If the vehicle leaves Titan's atmosphere at that time, it will fall directly into Saturn beginning with zero velocity of the Titan orbit. The low entry velocity into Saturn's atmosphere could enable an interesting long duration exploration of the atmosphere using the inherent high-lift capabilities of the waverider as a gliding entry vehicle. If the vehicle remains in Titan's atmosphere, the drag loss would continue to slow the vehicle until its velocity was below the escape velocity of Titan and the vehicle would be captured in a Titan orbit. In addition, the maneuver ability of the waverider would allow inclination changes that could result in a polar orbit about Titan that has been shown[8] to have long term stability.

The Titan B case illustrates a nearly orthogonal initial relationship between $V_S$ and $T_S$ allowing the typical rotations shown. These rotations could enable major redirections of the $V_S$ vector to facilitate other satellite encounter trajectories. (Note that the Titan B case is only approximate because the $V_S$ and $T_S$ vectors would never be exactly orthogonal at that location in Titan's orbit.) The Titan C case suggests that rotation of the $V_\infty$ vector (out of plane in this case) through less than 90 deg would provide a $V_S$ vector orthogonal to the satellite motion (i.e., a Saturn polar orbit). The Titan D case is similar to the Titan B case, but the initial orthogonality could be exact (i.e., a rectilinear approach trajectory to Saturn).

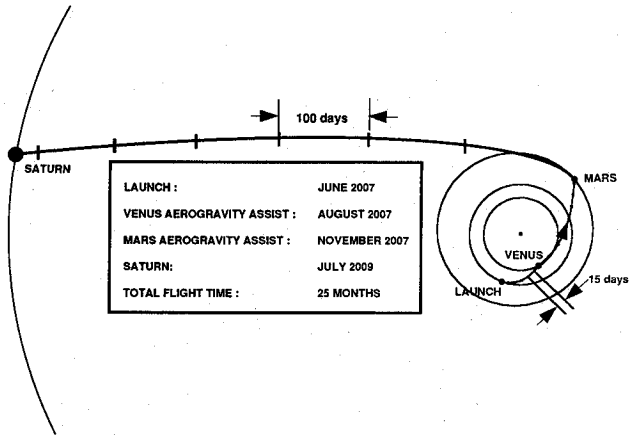


Fig. 7 VAGAMAGA trajectory to Saturn.

## Missions to Uranus and Neptune

To get the most $\Delta V$ from Mars, the AGA maneuver at Mars would be performed at about the technology limit of AGA atmospheric speed. At present this is believed to be 15 km/s, arising from a $V_{\text{inf}M}$ of about 14 km/s. The flight time[3] from Mars to Saturn, Uranus, and Neptune as a function of $V_{\text{inf}M}$ is shown in Fig. 9, and the $V_{\text{inf}}$ at the target planet[3] is shown

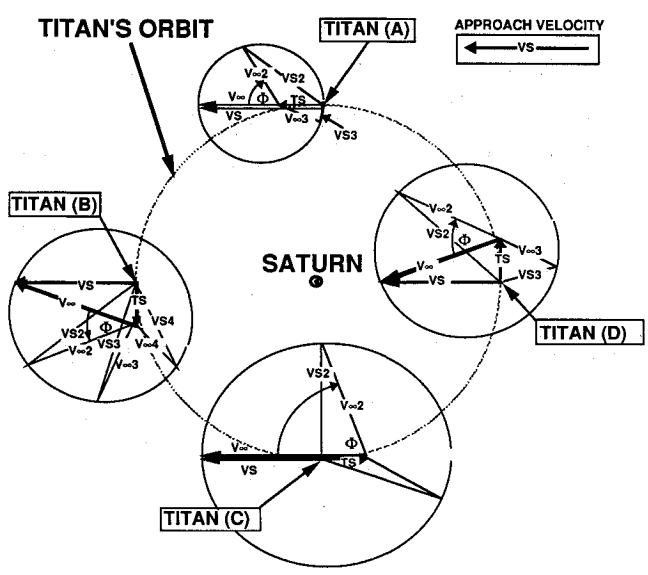


Fig. 8 Titan aerogravity-assist (TAGA) maneuver possibilities.

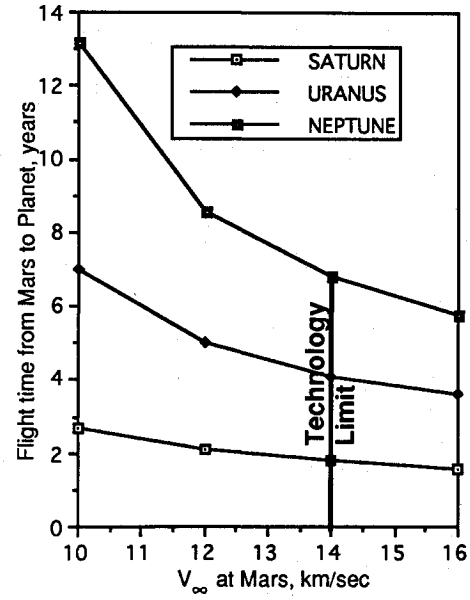


Fig. 9 Flight duration to the outer planets.

in Fig. 10. It can be seen that for $V_{infM} = 14$ km/s the flight time to Uranus and Neptune is about 4 and 7 yr, respectively, and the arrival $V_{inf}$ is about 19 and 18 km/s. The waverider vehicle could perform an aerocapture type of spiraling maneuver to go into orbit at the target planet, followed by a propellant burn to raise the periapsis. These speeds in the low MW gas of these outer planets are within the technology limit. The mission could include an atmospheric probe (although the waverider itself might be instrumented) that could be released on hyperbolic approach or after injection into orbit. The total travel time, including a time of about 0.2 yr (type 1) or 0.5 yr (type 2) for the Earth-to-Venus (E-V) part, and 0.3 yr for the Venus-to-Mars (V-M) part, is about 4.5–4.8 yr to Uranus and 7.5–7.8 yr to Neptune. One might compare these travel times with those for direct flight from Earth. Just to reach Neptune at 30 AU with a Hohmann transfer requires a $C_3$ of about 136 ($V_{infE} \approx 12$), and the flight time would be 30.6 yr. However, the missions currently being studied by NASA use some form of typical Jupiter gravity assist (GA, not AGA) and have a travel time of about 14 yr to Neptune and about 12 yr to Uranus.

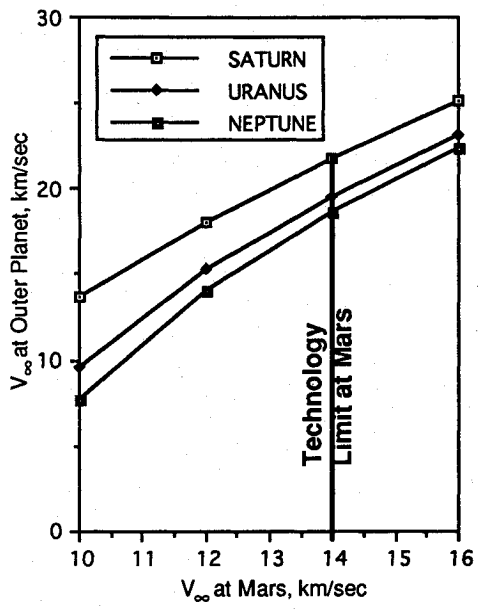


Fig. 10 $V_\infty$ at the outer planets vs $V_\infty$ at Mars.

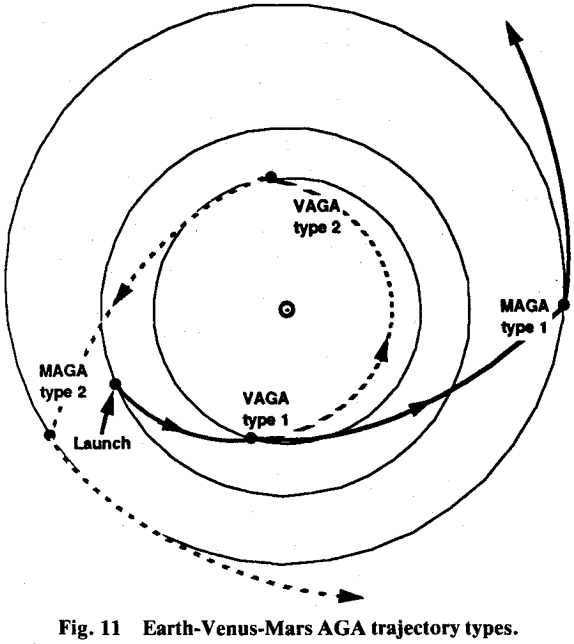


Fig. 11 Earth-Venus-Mars AGA trajectory types.

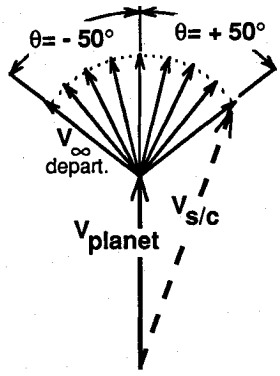


Fig. 12 Departure angle variation.

Thus AGA offers a considerable reduction in travel time to these planets even with the technology limitation.

## Mission Design Charts for VAGAMAGA Opportunities

In this section of the paper, a more conservative approach to AGA trajectories is taken. Constraints are imposed on launch velocity and atmospheric velocities at Venus and at Mars, and the effects of AGA velocity losses are evaluated. Here the data are developed more parametrically so that trends and sensitivities for the AGA trajectory concept can be more clearly understood along with the constrained technological assumptions.

Figure 11 illustrates the types of trajectories that include an AGA maneuver at Venus to go to Mars and an AGA at Mars to go to the outer planets. Type 1 or 2 trajectories have a transfer angle (from planet 1 to planet 2) of less than 180 deg or greater than 180 deg, respectively. We seek to determine the window of Earth launch opportunities, using two parameters as variables, the $V_\infty$ at departure and its direction relative to the planet's heliocentric velocity. Referring to Fig. 12, we varied this departure angle $\theta$ through a range of 50 deg on either side of the planet's velocity vector, at both Earth launch to go to Venus and for Venus departure to go to Mars. In doing this we are addressing the hypothesis that with AGA at Venus and Mars the launch $C_3$ at Earth is small and by varying $\theta$ we can increase the number of alignment opportunities for Earth-Venus-Mars trajectories. Figures 13–18 parametrically illustrate the data that are used to determine the opportunities, bending angles, drag losses, etc.

To be consistent with the concept of a technology limit on atmospheric velocities, the range of $V_\infty$ at Earth launch was restricted to give $V_p$ values (i.e., AGA atmospheric velocities) at Mars and Venus generally not exceeding 15 km/s. It was found that a consistent range of Earth launch $V_\infty$ values was about 4.6–6.6 km/s, i.e., a relatively low $C_3$ range of about 20–45 km$^2$/s$^2$. This would suggest a launch mass of as high as 7000 kg using the expected performance of the Titan/SRMU/Centaur in this decade. The range of Venus departing velocity $V_{\infty V}$ to go to Mars is about 7.8–9.8 km/s, to reach Mars with an approach velocity $V_{\infty M}$ of about 14 km/s (near the assumed technology limit). It will be convenient to show plots of the parameters ($\theta$ and $V_\infty$) for both these journeys: Earth to Venus (E-V) and Venus to Mars (V-M) simultaneously. The nomenclature will be to call the departure planet 1 and the arrival planet 2. It should be noted that these values are approximate, being derived for planets in assumed coplanar circular orbits, the advantage being that this analysis is independent of particular dates.

In Figs. 13–18, the abscissa is $\theta$, the departure angle between the $V_\infty$ vector and the planet's heliocentric velocity. The numerals within the figures are the values of the parameter $V_{inf1}$ for the various curves. Figure 13 shows the true anomaly (central angle at the Sun) range from launch to arrival for the E-V and V-M trajectories, as a function of the departure angle $\theta$,

varying from $-50$ to $+50$ deg, and $V_{inf1}$ varying as mentioned earlier. The nomenclature used here refers to the departure planet-arrival planet followed by a number denoting the type of trajectory between the two planets. Note that there are three sets of data: 1) type 1 transfers from Earth to Venus labeled E-V1, 2) type 2 transfers from Earth to Venus labeled E-V2, and 3) type 1 transfers from Venus to Mars labeled V-M1. (In addition, type 2 transfers from Venus to Mars, V-M2, exist, but their flight durations are many years as discussed below, not a "fast mission.") Clearly, the type 1 missions with the highest departure velocity $V_{inf1}$ at the first planet (either Earth or Venus) have the smallest change in relative true anomaly as illustrated typically in Fig. 13.

Figures 14 and 15 show the corresponding travel duration from body 1 to body 2, and the arrival $V_{inf2}$, as a function of the same variables $V_{inf1}$ and $\theta$. Note that Fig. 14 shows four sets of curves. Moving up from the bottom there are first two curves bounding the E-V1 case, with $V_{inf1}=6.6$ and 4.6 km/s. Then there are three curves for the V-M1 case, i.e., two bounding curves and one intermediate curve. Then there are two curves bounding the E-V2 case. The three curves located far above the others are for the V-M2 case. Again the durations on type 2 trajectories to Mars (V-M2) are on the order of years vs months for the other types.

Figure 16 shows the bending angles $\phi$ at Venus and Mars: the angle due to gravity alone (GRAV), the total required bending angle (TOTAL), to place the perihelion (i.e., $\theta=0$) of

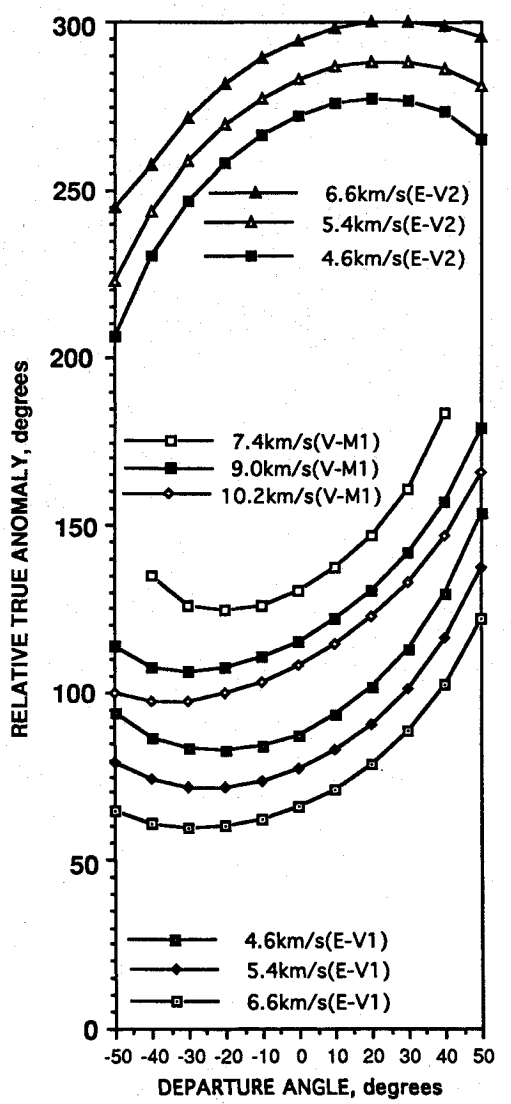


**Fig. 13 True anomaly of body 2 relative to body 1 vs departure angle $\theta$ for E-V1, E-V2, and V-M1 trajectories.**

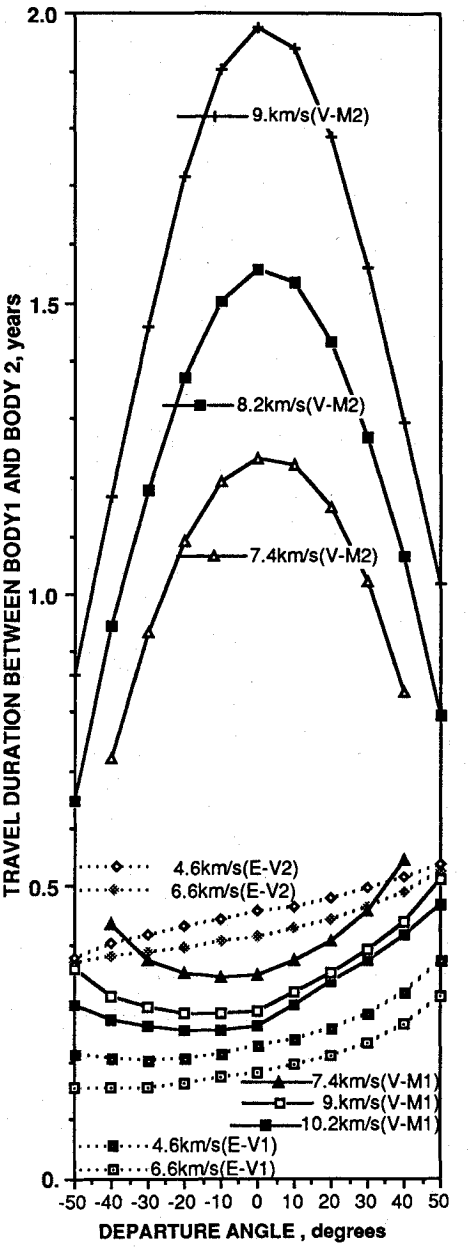


**Fig. 14 Travel time from body 1 to body 2 vs departure angle $\theta$ vs $V_\infty$.**

the departing trajectory at Venus and at Mars, and the difference (AERO), to be generated by the AGA maneuvers. Figure 16a shows three graphs of curves for Earth-to-Venus trajectories. The four curves near the top show the total bending angle to emerge with $\theta=0$, for four values of launch velocity. The four curves concave upwards near the center are the corresponding gravity turn angles, and the four flat-topped curves toward the bottom of the figure are the difference, i.e., the "aero" part of the turn. For Fig. 16b, the bending angle $\phi$ at Mars results in an interplanetary trajectory with the perihelion at Mars or $\theta=0$ at Mars.

Figure 17 shows the "aero" drag loss in AGA at Venus and Mars for a vehicle with $L/D=5$ on an Earth-Venus-Mars flight. The drag loss is shown as a function of the departure angle $\theta_1=-50$ to $+50$ deg at body 1, for an assumed $\theta_2=0$ leaving body 2. Typically, the aerobending angle would be the largest for the departure angle $\theta=0$ deg case (i.e., perihelion or aphelion at departure body) and the velocity loss would be the highest for this case. Three solid curves are shown for Venus, for three constant values of $V_\infty$ leaving Earth; similarly three

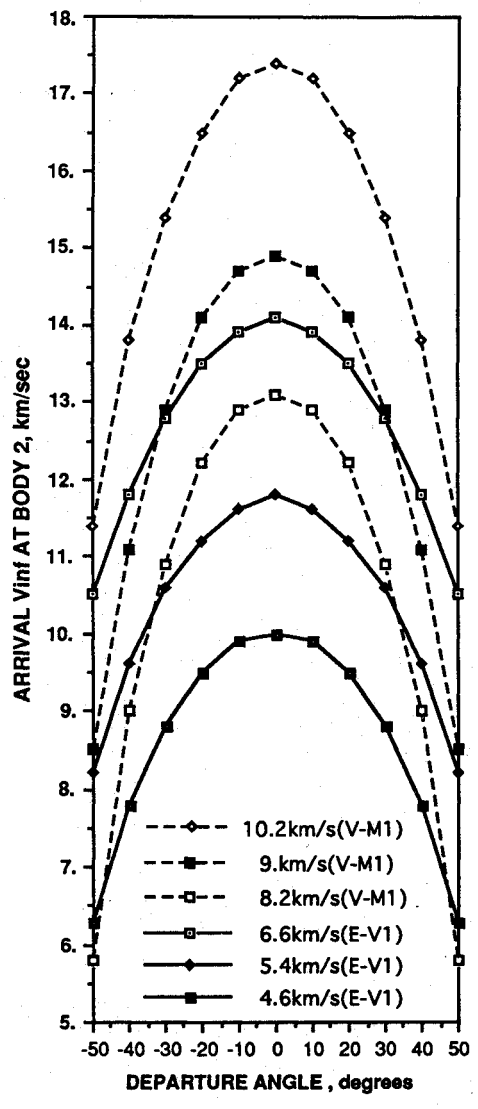


**Fig. 15 Arrival velocity at body 2 vs departure angle $\theta$ vs $V_\infty$.**

dashed curves are shown for Mars, for three constant values of $V_\infty$ leaving Venus.

## Planetary Alignment and Mission Opportunities

Figure 18 shows the relative celestial longitude ($CL$, central angle or true anomaly) of planet 2 relative to planet 1 at launch for these trajectory types, as a function of $V_{\text{inf1}}$ and $\theta_1$. Note that there are two opportunities to meet Venus in the trajectory from Earth (see Fig. 11), an inbound encounter, or type 1 (called E-V1), and an outbound encounter, or type 2 (E-V2). The durations for both are shown in Fig. 14; the other parameters are the same for type 2 as for type 1 because of symmetry. The figure shows four sets of curves. Starting at the top there are two curves that bound the range of $V_{\text{inf1}}$ examined for the V-M1 case. Then there are three curves, concave downwards, for the E-V2 case. Below that there are two curves for the E-V1 case, for $V_{\text{inf1}} = 4.6$ and 6.6 km/s. At the bottom part of the figure there are three curves of the V-M2 case, for $V_{\text{inf}V} = 8.2$, 9.0, and 10.2 km/s.

It can be seen from Fig. 16a that the mean (defined as $\theta = 0$) aerobending angle is about 50 deg at Venus, and from Fig. 16b it can be seen that the mean aerobending angle at Mars is about 60 deg (70 deg total minus 10 deg gravity bending). For $\theta = \pm 50$ deg, the aerobending angle would vary from zero (gravity bending alone would be enough) to about 100 deg (i.e., twice the mean) at Venus and to about 110 deg at Mars. Excessive aerovelocity loss may limit the possible aerobending angle. For the mean bending angle, the aerovelocity loss is (from Fig. 17) about 2–3 km/s at Venus and about 2–4 km/s at Mars. Examining Figs. 14 and 16, we note that a large aerobending angle (to get $\theta = 0$) is required at Venus from an E-V1 arrival, to go on a fast trip to Mars, and a smaller aerobending angle is required if we wish to go slowly to Mars following E-V2 to Venus. Again, at Mars a small aerobending angle is required if we place perihelion inside the Mars orbit and are outbound from Mars.

The data of Figs. 12, 13, and 18 are used here to construct example cases in Table 1 and Fig. 19. Tabulated data (see Table 1) have been generated for typical trajectory cases between two planets (i.e., E-V1, E-V2, and V-M1) and three planets (E-V-M). The two-planet cases include both fast (e.g., E-V1 fast) and slow (e.g., E-V1 slow) trajectories. The second column in Table 1 lists the total transfer angle of a trajectory case from the launch to the final planet. Note that for cases 9–20 this is the transfer angle between Earth and Mars. Column 3 of the table lists the total travel time between Earth and the final planet. The difference between the celestial longitude of the final planet and the longitude of the initial planet is given in column 4 at the time of departure from the initial planet. Note that the Earth is the initial planet in all of the cases except cases 7 and 8. Finally, column 5 in the table lists launch years for some of the cases. Using these data, it is possible to find the range of Venus and Mars celestial longitudes relative to Earth at Earth launch, i.e., windows of Earth-relative geometry to reach these planets in the range of variables $V_{\text{inf}E}$ and $\theta$ analyzed.

To identify VAGAMAGA mission opportunities to the outer planets, it is necessary to determine if the AGA at Mars occurs for Mars positioned suitably for a mission to a specific outer planet after Mars AGA. The second column of Table 1 for cases 9–20 can be interpreted as the $CL$ at MAGA relative to the $CL$ of the Earth at launch time. If we plot cases 9–20 on a polar grid as shown in Fig. 19 (e.g., case 9 is 160 deg measured from $E_0$), the greatest gap between $CL$ (at MAGA) is 94 deg for cases 9 and 11; the next greatest is 48 deg between cases 10 and 13. We note that the values cycle 360 deg for the Mars/Earth synodic period (2.135 yr), so that the longest time for which one would have to delay an Earth launch would be $94/360 \times 2.135$ yr $= 0.56$ yr or about 6.7 months. One should note that about 20 deg or so of heliocentric steering could be done at Mars AGA exit to aim for the desired outer planet, so

**Table 1 Example numerical data for VAGAMAGA trajectories**

| Case | Total transfer angle, deg | Total travel time, yr | $\Delta CL(f/i)$,[a] deg | Sample launch year |
|---|---|---|---|---|
| 1. E-V1 fast | 60 | 0.156 | −27.1 (G) | 2007 |
| 2. E-V1 slow | 154 | 0.375 | −65.7 (L) | |
| 3. E-V2 fast | 206 | 0.379 | −15.1 | |
| 4. E-V2 fast | 249 | 0.372 | −27.1 | |
| 5. E-V2 medium | 294 | 0.415 | 51.5 (G) | 2006 |
| 6. E-V2 slow | 265 | 0.537 | −48.8 (L) | |
| 7. V-M1 fast | 100 | 0.299 | 42.6 | |
| 8. V-M1 slow | 198 | 0.597 | 83.8 | |
| 9. E-V-M 1+7 | 160 | 0.455 | 73 | 2007 |
| 10. E-V-M 1+8 | 258 | 0.753 | 114 | |
| 11. E-V-M 2+7 | 254 | 0.674 | 125 | |
| 12. E-V-M 2+8 | 352 | 0.972 | 166 | |
| 13. E-V-M 3+7 | 306 | 0.678 | 176 (L) | 2006 |
| 14. E-V-M 3+8 | 404 | 0.976 | 217 | |
| 15. E-V-M 4+7 | 349 | 0.671 | 221 | |
| 16. E-V-M 4+8 | 447 | 0.969 | 262 | |
| 17. E-V-M 5+7 | 394 | 0.614 | 276 | |
| 18. E-V-M 5+8 | 492 | 1.012 | 298 (G) | 2006 |
| 19. E-V-M 6+7 | 365 | 0.836 | 205 | |
| 20. E-V-M 6+8 | 463 | 1.134 | 246 | |

[a] $\Delta CL(f/i)$ = celestial longitude of final planet relative to initial planet at time of departure from initial planet. In cases 9–20, the initial planet is Earth, the final planet is Mars. Notations L and G indicate least and greatest $CL$ in range examined.

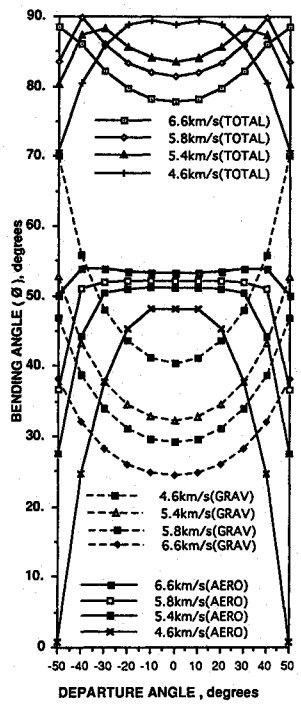


**Fig. 16a Bending angles $\phi$ at Venus vs departure angle $\theta$ at Venus vs launch velocity for E-V trajectories.**

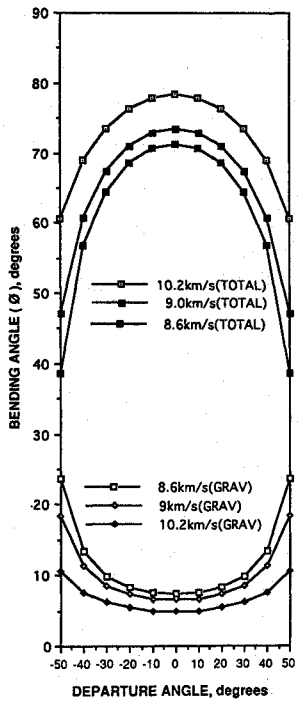


**Fig. 16b Bending angles $\phi$ at Mars vs departure angle $\theta$ at Mars vs departure $V_\infty$ at Venus for V-M trajectories.**

that the 94 deg could be reduced to about 74 deg (delay of 0.44 yr or 5.3 months).

In Fig. 20 the line marked E-V1 shows all of the opportunities (in the 16 years shown) for the example cases 1 and 2 of Table 1, and the line marked E-V2 shows all of the opportunities for example cases 5 and 6. The lines marked (E-V1)-M show all of the opportunities for cases 9–12, and the lines marked (E-V2)-M show all opportunities for cases 13–18. The time represented by the horizontal bars in Fig. 20 can be considered "windows" for Earth launch because of the several cases that fall there and the fact that one can "steer" the AGA exit at Mars to construct a continuously variable exit heliocentric direction (within the constraints discussed previously).

Launch opportunities to the far outer planets using VAGAMAGA trajectories are shown in Fig. 20. The tics on the three dashed lines at the bottom of each figure identify the opportunities (from this preliminary analysis) that exist for a Mars departure trajectory that is aligned with the given outer planets. Note that at least two outer planet trajectories exist at each of the VAGAMAGA launch opportunities. The figure illus-

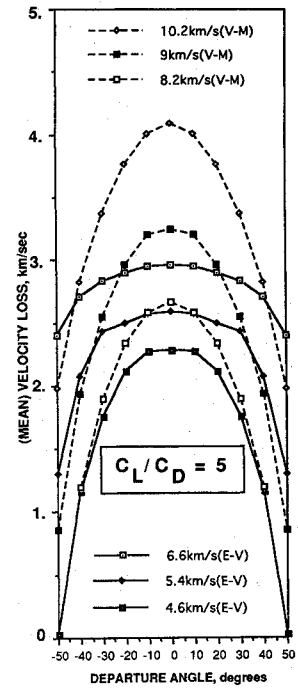


**Fig. 17 Velocity loss in AGA maneuver at body 2 vs departure angle $\theta$ at body 1 vs departure $V_\infty$ at body 1 for $L/D = 5$**

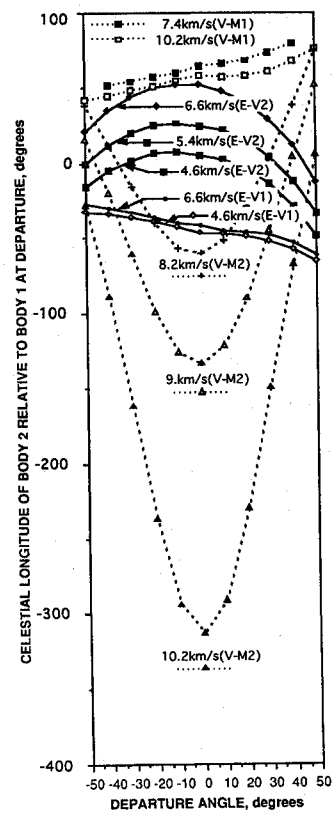


**Fig. 18 Relative celestial longitude of bodies vs departure angle $\theta$ vs $V_\infty$.**

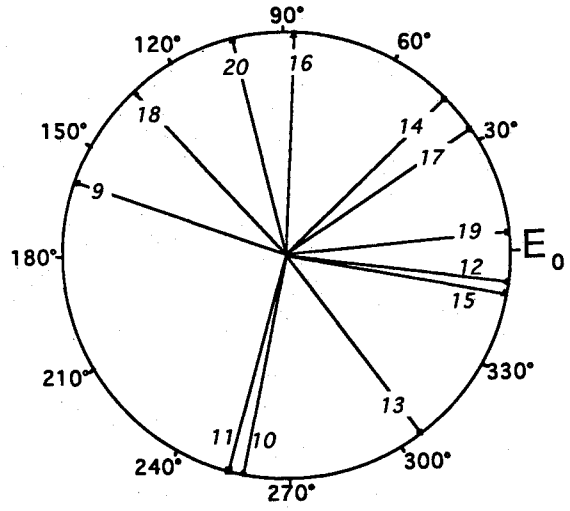


**Fig. 19 Celestial longitude of Mars relative Earth launch longitude ($E_0$) for VAGAMAGA trajectory cases 9–20 from Table 1.**

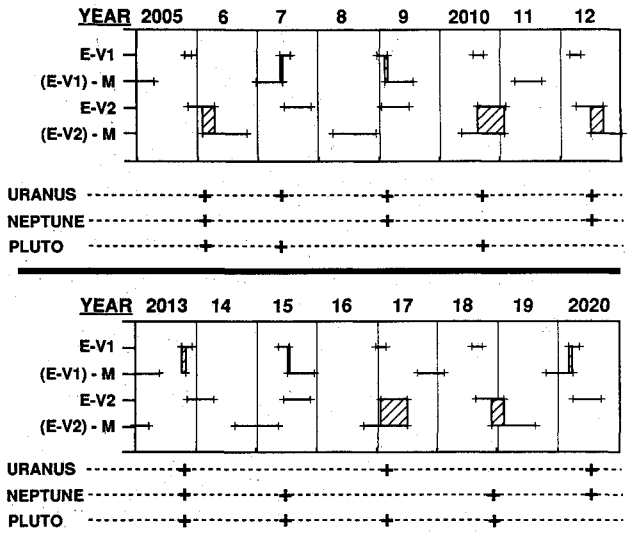


**Fig. 20 Positions of the terrestrial planets and launch opportunities to the far outer planets from 2005–2020.**

trates data analysis exemplified in Table 1 (note the launch dates in column 5 of Table 1) but corresponding to all of the windows for VAGAMAGA trajectories in calendar time in the interval 2005–2020. In the figure, if an E-V1 window coincides with an (E-V1)-M window, the opportunity exists for an E-V-M or VAGAMAGA opportunity. As shown in the figure, there are E-V opportunities every E-V synodic period (1.6 yr). Of these, an E-V1 trajectory pair in succession (e.g., 2007 and 2009) will give an E-V-M opportunity, and then the next two (e.g., 2010 and 2012) will not. The same is true for the E-V2 trip, the result being that an E-V-M opportunity exists every 1.6 yr. Since the Earth-Mars synodic period is 2.135 yr, the celestial longitude of Mars at MAGA rotates 107 deg in 1.6 yr. If one could not control this, the AGA at Mars would likely be favorable for a trip to the outer planets only every 3 or 4 occasions. However, the range of control of arc (Table 1: cases 9–12 or 160–352 deg via E-V1 and cases 13–18 or 306–492 deg via E-V2) and of $\theta$ at Mars departure seems large enough so that one could arrange AGA at Mars to be favorably located for flight to at least one outer planet at every 1.6 yr opportunity as shown.

In the second decade of the next century the far outer planets will be positioned such that Uranus is "ahead" of Neptune in celestial longitude (also, Neptune is ahead of Pluto). Thus, retrograde heliocentric trajectories would be suggested if single missions to multiple planets (i.e., "grand tours") were contemplated. Retrograde flybys of each planet would clearly reduce the heliocentric velocity and lengthen the flight durations between the far outer planets.

It should be noted that a direct Earth-to-Mars trajectory with an AGA to go to the outer planets is also a viable mission. There would be a trade of simplicity and opportunity vs $C_3$ at Earth launch. For example, with a VAGAMAGA trajectory, a $V_{\text{inf}M}$ at Mars of 14 km/s (technology limit) is attained by a $V_{\text{inf}V}$ of 6.6 km/s at Venus (corresponding to a $V_{\text{inf}V}$ arrival of about 7.6 km/s), achieved with a $V_{\text{inf}E}$ of 3.8 km/s launch velocity. A direct trajectory from Earth to Mars (E-M) would arrive at Mars with $V_{\text{inf}M} = 14$ km/s for a $V_{\text{inf}E}$ of about 7.9 km/s launch velocity. Thus, a $C_3$ of about 60 (Titan-Centaur launch mass ~ 3500 kg) is required for the E-M flight, compared with a $C_3$ of about 15 (launch mass ~ 7500 kg) for the E-V-M flight. On the other hand, the Earth-Mars geometry repeats about every 2.1 years, and Mars repeats its position relative to the outer planets every 1.88+ yr. Since the periods of Uranus and Neptune (about 84 and 165 yr) are large, they move slowly, so that AGA at Mars to go to Uranus or Neptune would be available for two successive revolutions of Mars, and it takes about 7 revolutions to return to an initial configuration relative to Earth and the outer planets.

## Conclusions

The AGA techniques offers flexibility in mission design that is not possible with GA alone. Using GA alone here is a limit on the approach velocity to a small planet like Venus because the available bending decreases as the velocity increases. With the AGA technique, considerably higher velocities are possible and the limit on velocity is the technology of the atmospheric flight. AGA also offers flexibility of turn angle over a considerable range, whereas GA is flexible (by adjusting flyby distance) up to the limit consistent with the velocity. Another difference is that Mars can be used quite effectively for an AGA maneuver, whereas its mass is too low to contribute much bending in a GA maneuver.

The development of the AGA technique has evolved from early studies that considered no technology constraints to the current analyses that include some of these constraints. The results suggest that, even accepting these relatively conservative performance constraints, there are trajectories to the planets with significant performance improvements over typical GA or direct trajectories. In addition, parametric trajectories have been examined from Earth to Venus and from Venus to Mars, varying the departure $V_\infty$ and the departure angle relative to the planet's heliocentric velocity. It has been established that a range of $C_3$ at Earth of about 20–50 km$^2$/s$^2$ and a variation of $\pm 50$ deg in $V_\infty$ departure angle will provide a window of about 93 deg in the celestial longitude of Venus at Earth launch for an E-V1 trajectory and about 100 deg for E-V2. With a similar range of $\theta$ at Venus departure and the range of $V_{\text{inf}V}$ appropriate to the arrival conditions (less velocity loss), one can reach Mars at each Earth-Venus opportunity. The sequence of opportunities would be two E-V1 trajectories, followed by two E-V2 trajectories, and so on. Further, it is likely that typically one can arrange AGA maneuvers at Mars where Mars is favorably located for a trajectory to at least one of the far outer planets every 1.6 years. Using the waverider for aerodynamic maneuvers at the outer planets could yield new mission possibilities such as orbit insertion at the planets and maneuvers at Titan that yield unique mission opportunities within the Saturn system.

## Acknowledgments

This research was performed by the Jet Propulsion Laboratory, California Institute of Technology, under contract with NASA.

## References

[1]Randolph, J. E., and McRonald, A. D., "Solar Probe Mission Status," American Astronautical Society, AAS Paper 89-212, April 1989.

[2]McRonald, A. D., and Randolph, J. E., "Hypersonic Maneuvering to Provide Planetary Gravity Assist," AIAA Paper 90-0539, Jan. 1990.

[3]McRonald, A. D., and Randolph, J. E., "Applications of Aero-Gravity-Assist to High Energy Solar System Missions," AIAA Paper 90-2891, Aug. 1990.

[4]Anderson, J. D., and Lewis, M., "Hypersonic Waveriders for Planetary Atmospheres," AIAA Paper 90-0538, Jan. 1990.

[5]Anderson, J. D., Lewis, M. J., Corda, S., Blankson, I. M. (eds.), *Proceedings of the 1st International Hypersonic Waverider Symposium,* Dept. of Aerospace Engineering, Univ. of Maryland, College Park, MD, Oct. 1990.

[6]Lewis, M. J., and McRonald, A. D., "The Design of Hypersonic Waveriders for Aero-Assisted Interplanetary Trajectories," AIAA Paper 91-0053, Jan. 1991.

[7]Elliot, J. L., Dunham, E. W., Bosh, A. S., Slivan, S. M., Young, L. A., Wasserman, L. H., and Millis, R. L., "Pluto's Atmosphere," *Icarus,* Vol. 77, 1989, pp. 148-170.

[8]Friedlander, A., personal communication, Aug. 1990.

Ernest V. Zoby
*Associate Editor*